CANCER GENOMICS & PROTEOMICS *19*: 692-702 (2022)
doi:10.21873/cgp.20352

TMED9 Expression Level as a Biomarker of Epithelial Ovarian Cancer Progression and Prognosis

GWAN HEE HAN[1], HEE YUN[2], JOON-YONG CHUNG[3], JAE-HOON KIM[4,5] and HANBYOUL CHO[4,5]

[1]*Department of Obstetrics and Gynecology, Kyung Hee University Hospital at Gangdong, Seoul, Republic of Korea;*
[2]*Department of Obstetrics and Gynecology, Gangnam Severance Hospital, Yonsei University College of Medicine, Seoul, Republic of Korea;*
[3]*Molecular Imaging Branch, Center for Cancer Research, National Cancer Institute, National Institutes of Health, Bethesda, MD, U.S.A.;*
[4]*Department of Obstetrics and Gynecology, Yonsei University College of Medicine, Seoul, Republic of Korea;*
[5]*Institute of Women's Life Medical Science, Yonsei University College of Medicine, Seoul, Republic of Korea*

Abstract. *Background: Transmembrane emp24 domain-containing protein 9 (TMED9) belongs to the TMED/p24 family that transports, modifies, and packs proteins and lipids into vesicles for delivery to specific locations and is important in innate immune signaling via the endoplasmic reticulum–Golgi cargo pathway. TMED9 has been implicated in various cancer types; however, its role in epithelial ovarian cancer (EOC) is unclear. In this study, we aimed to elucidate the role and clinical significance of TMED9 in EOC. Materials and Methods: mRNA and protein levels of TMED9 and their associations with clinicopathological features in EOCs were evaluated using RNA-sequencing and immunohistochemistry data. Functional studies assessing the tumorigenic role of TMED9 in EOC cell lines were also performed. Results: The mRNA expression of TMED9 was up-regulated in EOC compared to that in normal ovarian epithelium. TMED9 protein expression increased in progression from normal ovarian epithelium to EOC ($p<0.001$). Moreover, high expression of TMED9 was associated with advanced stage, serous cell type and poor histological grade in EOC and demonstrated independent prognostic significance for both disease-free and overall survival. Further functional studies showed that TMED9 knockdown reduced migration, invasion, cell proliferation, and colony formation of EOC cells. Conclusion: Overall, our results support the use of TMED9 as a valuable prognostic biomarker and provide evidence for targeting of TMED9 as a novel strategy for EOC treatment.*

Correspondence to: Professor Hanbyoul Cho (ORCID ID: 0000-0002-6177-1648), MD, Ph.D., Department of Obstetrics and Gynecology, Gangnam Severance Hospital, Yonsei University College of Medicine, 211 Eonju-Ro, Gangnam-Gu, Seoul 06273, Republic of Korea. Tel: +82 220193430, Fax: +82234628209, e-mail: hanbyoul@yuhs.ac

Key Words: TMED9, ovarian cancer, biomarker. prognosis, diagnosis.

This article is an open access article distributed under the terms and conditions of the Creative Commons Attribution (CC BY-NC-ND) 4.0 international license (https://creativecommons.org/licenses/by-nc-nd/4.0).

Epithelial ovarian cancer (EOC) is one of the most prevalent and fatal malignant carcinomas of the female population with approximately 21,410 new cases and 13,770 cancer-related deaths in 2021 in the United States alone (1, 2). A progressive rise in the occurrence of EOC in South Korea, with 3,080 new cases and 1,344 fatalities in 2021, has been attributed in part to the westernization of lifestyles and changes in reproductive variables (3).

Platinum-based adjuvant chemotherapy after performing debulking surgery is the mainstay of EOC management, with an effective response rate in more than 90% of patients. However, the 5-year survival rate of patients with EOC remains low at approximately 40%, and there has only been modest improvement in the past decades despite the advent of antiangiogenic drugs and poly adenosine diphosphate-ribose polymerase inhibitors (4-7). The unfavorable prognosis of EOC is attributed to the lack of effective clinical screening methods in the early stages of the disease, resulting in diagnosis at advanced stages. Thus, to reduce disease mortality, it is crucial to develop early detection methods targeting diagnostic biomarkers and therapeutic strategies of EOC to improve the prognosis of patients.

Transmembrane emp24 domain-containing protein 9 (TMED9) belongs to the TMED/p24 family, which are important protein transport regulators involved in delivery of proteins to targeted destinations *via* the endoplasmic

reticulum (ER)-Golgi cargo pathway (7-9). To date, studies on TMED proteins suggest that dysregulation in protein transport *via* the ER-Golgi cargo pathway alters cell proliferation and differentiation and contributes to diseases, especially cancer. For example, overexpression of *TMED9* was reported to promote cell proliferation, migration, and invasion of hepatocellular carcinoma (HCC) cells by increasing the expressions of β-catenin and GLI family zinc finger 1 (*GLI1*); TMED9 was identified as a poor prognostic and prognosis predictive biomarker in patients with HCC (10). Sonakshi *et al*. reported that overexpression of *TMED9* promoted colon cancer metastasis by driving the cornichon family α-amino-3-hydroxy-5-methyl-4-isoxazole propionic acid receptor auxiliary protein 4 (CNIH4)/transforming growth factor alpha (TGFα)/GLI family zinc finger signaling pathway while inhibiting the TMED3-Wingless-related integration site (WNT)-transforming growth factor signaling pathway (11). Additionally, overexpression of *TMED9* promoted breast cancer cell proliferation and migration and was identified as a potential prognostic biomarker and drug target for breast cancer (12). However, at present, there is little evidence supporting the role of *TMED9* in EOC.

Therefore, in the present study, we aimed to elucidate the role of *TMED9* in EOC and provide a theoretical basis for the clinical application of *TMED9* in the diagnosis and treatment of EOC by analyzing its mRNA expression pattern in EOCs and normal ovarian epithelial tissues using RNA-sequencing (RNA-seq) data and data from multiple public cohorts. Additionally, we investigated the protein expression pattern of TMED9 in EOCs using immunohistochemistry (IHC) and analyzed its relationship with clinicopathological parameters. The effect of TMED9 on proliferation and metastatic capacity was evaluated in several EOC cell lines to identify the functional role of *TMED9* in EOC.

Materials and Methods

Patients and tumor specimens. Tissue samples were obtained from patients who underwent primary cytoreductive surgery at the Gangnam Severance Hospital between 1996 and 2012 and the Korean Gynecologic Cancer Bank as part of the Bio and Medical Technology Development Program of the Ministry of the National Research Foundation. A total of 417 tissue samples (namely 212 EOCs, 52 borderline tumors, 83 benign tumors and 70 non-adjacent normal ovarian epithelia) were included in the study. The clinical information of the patients, including age, International Federation of Gynecology and Obstetrics (FIGO) stage, (13) histological classification of tumors based on the World Health Organization grading system (14), surgical procedure, response to platinum-based chemotherapy, examine medical records and pathology reports, data on serum levels of cancer antigen 125 (CA-125), survival duration, and survival status were gathered from electronic medical record. All patients underwent a maximum cytoreductive procedure, then received paclitaxel/carboplatin-based adjuvant chemotherapy. From the date of surgery to the time of relapse or the last follow-up consultation, disease free-survival (DFS) was assessed using the Response Evaluation Criteria in Solid Tumors (RECIST; version 1.1), which is based on the patient's response to therapy determined through spiral computed tomography or positron emission tomography – computed tomography (15). Overall survival (OS) was assessed from the date of surgery to either the patient's death or the date of last follow-up consultation with living patients. In compliance with the provisions of the Institutional Review Board (IRB) of Gangnam Severance Hospital, all tumor tissues were histologically investigated by a gynecologic pathologist, and all biological specimens were collected after securing informed consent from the participants (IRB No. 3-2020-0377).

Tissue microarray (TMA) and immunohistochemistry. A TMA was constructed with tissue cores of 1.0 mm in diameter containing a sufficient proportion of tumor cells punched from the donor formalin-fixed paraffin-embedded (FFPE) tissues or tissue blocks using a tissue arrayer (Beecher Instruments, Inc., Silver Spring, MD, USA). The TMA blocks were cut to 5-μm thickness using a rotary microtome. After sectioning, TMA sections were deparaffinized with xylene and rehydrated in serially graded ethanol to distilled water. Antigen retrieval was performed by incubating the TMA sections in a steam pressure cooker (Pascal; Dako, Carpinteria, CA, USA) containing heat-activated antigen retrieval buffer (Dako) at pH 6.0 for anti-TMED9 (rabbit polyclonal antibody, cat. #HPA014650, 1:100; Sigma-Aldrich Co. LLC, St. Louis, MO, USA), and a 3% H_2O_2 solution in methanol was used to treat the sections for 10 min to block endogenous peroxidase activity. The slides were stained for 30 min at room temperature with anti-TMED9 after being rinsed. Subsequently, the antigen-antibody reactions were visualized using Envision+ Dual Link System-HRP (Dako) and DAB+ (3,3'-diaminobenzidine; Dako) for 10 min. The stained slices were deposited in Faramount aqueous mounting solution after being dehydrated, counterstained with hematoxylin, (Dako). Appropriate negative and positive controls were also included.

Evaluation of IHC staining of TMA. A high-resolution optical was used to capture images of the stained TMA sections. (NanoZoomer 2.0 HT; Hamamatsu Photonics K.K., Hamamatsu City, Japan) at 20× objective magnification (0.5 μm resolution). Utilizing Visiopharm software, version 6.5.0.2303 (Visiopharm, Hrsholm, Denmark), the scanned sections were analyzed. On a scale of 0 to 3, the intensity of the brown staining was rated (0=negative, 1=weak, 2=moderate, and 3=strong) and the percentage of cytoplasm-stained tumor cells (range=0-100) was obtained using a predefined optimized algorithm. The total histoscore was determined by multiplying the percentage of positively stained cells by the intensity score (score range=0-300).

Laser-capture microdissection and RNA extraction and quality control. Hematoxylin and eosin were used to stain all FFPE tissue slides, and an experienced gynecological pathologist reviewed the slides. A Leica AS LMD laser microdissection system (Leica Microsystems Inc., Buffalo Grove, IL, USA) was used according to the manufacturer's instructions to perform a laser-capture microdissection where the desired lesions were cut out from the tissue. The sectioned FFPE tissues were placed on slides with a polyethylene terephthalate membrane (Leica Microsystems, Inc., Buffalo Grove, IL, USA). TRIzol reagent (Invitrogen, Gaithersburg, MD, USA) was used to isolate total RNA, and the quality of the

RNA was measured with an Agilent 2100 bioanalyzer using an RNA 6000 Nano Chip (Agilent Technologies, Amstelveen, Netherlands). An ND-2000 spectrophotometer (Thermo Scientific, Wilmington, DE, USA) was used for RNA quantification.

Library preparation and sequencing. For control and test RNAs, library construction was performed using the QuantSeq 3' mRNA-Seq Library Prep Kit (Lexogen, Inc., Austria), according to the manufacturer's instructions. Briefly, 500 ng of total RNA was prepared for the control and experimental RNAs. RNA was hybridized with an oligo-dT primer, including an Illumina-compatible sequence at its 5' end. Reverse transcription was performed, and after the RNA template was degraded, a random primer with an Illumina-compatible linker sequence at its 5' end was used for second-strand synthesis. Magnetic beads were used to purify the double-stranded library. To perform cluster generation, complete adapter sequences were added to this library, and polymerase chain reaction components were removed from the final library. NextSeq 500 (Illumina, San Diego, CA, USA) was used for single-end 75-base pair high-throughput sequencing.

RNA sequencing read mapping and gene expression analysis. Through sequencing, we obtained FASTQ raw data for eight independent libraries for both platinum-sensitive and platinum-resistant strains; in total, 16 samples were obtained. All FASTQ reads were trimmed and adapters were removed for quality control using BBduk (BBMap v36.59) (16) and FASTQC (v0.11.7) (17) for the sequencing data. We carried out mapping through the STAR-HTSeq workflow, that is, STAR (v2.7.3a) (v2.7.3a) (18) and HTSeq-count (v0.12.4) (19), where the reference genome (GRCh38) and annotations were aligned to the sequencing reads. After quantifying read counts, we performed normalization and differential expression analyses on the levels of gene expression using the DESeq2 v1.26.0 R package (20) where normalization method was applied as a variance-stabilizing transformation. We selected differentially expressed genes (DEGs) that satisfied two different criteria: i) Adjusted $p<0.05$ (*i.e.*, Benjamini and Hochberg method) and ii) absolute $\log_2$ fold-change >2).

Public database. To validate our RNA-seq data, three datasets [GSE190688 (21), GSE54388 (22), GSE 40595 (23)] that analyzed DEGs between normal and high-grade serous ovarian cancer (HGSOC) samples were downloaded from the GEO Database (https://www.ncbinlm.nih.gov/geo/, accessed on December 20, 2021). An online public database, Kaplan–Meier Plotter (http://www.kmplot.com) which contains 10,293 lung, breast, gastric, and ovarian cancer samples to evaluate clinical outcomes of 54,675 genes were used to verify the prognostic significance of TMED9. A PostgreSQL serving running the web tool is able to combine clinical and gene-expression data and information (24).

Cell lines and culture. The American Type Culture Collection (Manassas, VA, USA) and the European Collection of Cell Cultures (Salisbury, UK) provided the primary ovarian cancer cell lines OVCAR3 and A2780, respectively. From the Korea Cell Line Bank, SNU840 cells were obtained (Seoul, Republic of Korea). OVCA433 cells were obtained from the Catholic University of Korea at St. Vincent Hospital. RMUG-S was obtained from the Japanese Collection of Research Bioresources Cell Bank (Osaka, Japan). In Dulbecco's modified Eagle medium treated with 10% fetal bovine serum (FBS) and 1% penicillin/streptomycin, ovarian cancer cells were grown. Two immortalized HOSE cell lines (IHOSE4138 and 8695) were established previously (25) and kept in Dulbecco's modified Eagle's medium with 10% FBS and 50 μg/ml gentamicin as supplements. All cell lines were incubated at 37˚C in a humidified incubator with 5% CO_2.

siRNA transfection. Bioneer supplied the targeted small interfering RNAs (siRNAs) against TMED9 and the reference siRNA (Daejeon, Republic of Korea). The following were the siRNA combinations: TMED9 #1, 5'-GUGAACAUGCCAAUGACUA-3' (sense) and 5'-UAGUCAUUGGCAUGUUCAC-3' (antisense); TMED9 #2, 5'-GUGCAAGUGACUCAGUCAU-3' (sense) and 5'-AUGACUGA GUCACUUGCAC-3' (antisense). Cells grown in 6-well plates were transfected with siRNA utilizing Lipofectamine® RNAiMAX Reagent (Invitrogen, Gaithersburg, MD, USA) as directed by the manufacturer, at a final concentration of 100 pmol per well.

Western blot analysis. Phenylmethylsulphonyl fluoride was administered to a cell lysis buffer (Cell Signaling Technology, Danvers, MA, USA) before the samples were extracted and lysed. Sodium dodecyl sulphate-polyacrylamide gel electrophoresis was used to separate the proteins from the cell lysates and deposit them onto a nitrocellulose membrane. Antibodies against TMED9 and α-actinin were purchased from Atlas Antibodies AB (Bromma, Sweden) and Santa Cruz Biotechnology (Santa Cruz, CA, USA), respectively. Enhanced chemiluminescence substances were used to see the immunoreactive bands (Thermo Fisher Scientific, Waltham, MA, USA).

Cell proliferation assay. Cell proliferation of each cell line was measured using an EZ-Cytox assay kit (Daeil Lab Service, Seoul, Republic of Korea), according to the manufacturer's instructions. Using a microplate reader, the intensity for each well was determined at 450 nm, and the study was performed in triplicate (Bio-Rad Laboratories, Inc., Hercules, CA, USA).

Colony-formation assay. OVCAR3 and OVCA433 cells were transfected with siRNA targeting *TMED9*. After 48-h transfection, 500 cells per well were planted into a 6-well plate and the cells were kept in an incubator at 37˚C with 5% CO_2 for 2 weeks. The plates were stained with 0.5% crystal violet for 30 min after being fixed with methanol for 10 min. Colonies were counted under a microscope after being rinsed with distilled water. A colony was only counted only when a single clone contained more than 100 cells. The experiment was performed three times.

Boyden chamber assay. Microchemotaxis chambers (Neuro Probe, Gaithersburg, MD, USA) with 48 wells were utilized to assess cell invasion. The bottom cells were filled with culture medium containing 10% FBS before being overlaid with Matrigel-coated membranes (#PFB8; Neuro Probe) from BD Biosciences (San Jose, CA, USA). The upper cells were seeded with siRNA-transfected cells (1×10^5 cells/50 μl of medium containing 0.05% FBS). The membranes were fixed and dyed with Diff-Quick solution after 24 h (Sysmex, Kobe, Japan). An Axio Imager M2 microscope was used to extract the cells from the membrane's top surface and measure the invader cells in six randomly selected high-power field for each filter (Carl Zeiss, Thornwood, NY, USA). Three times the experiment was conducted.

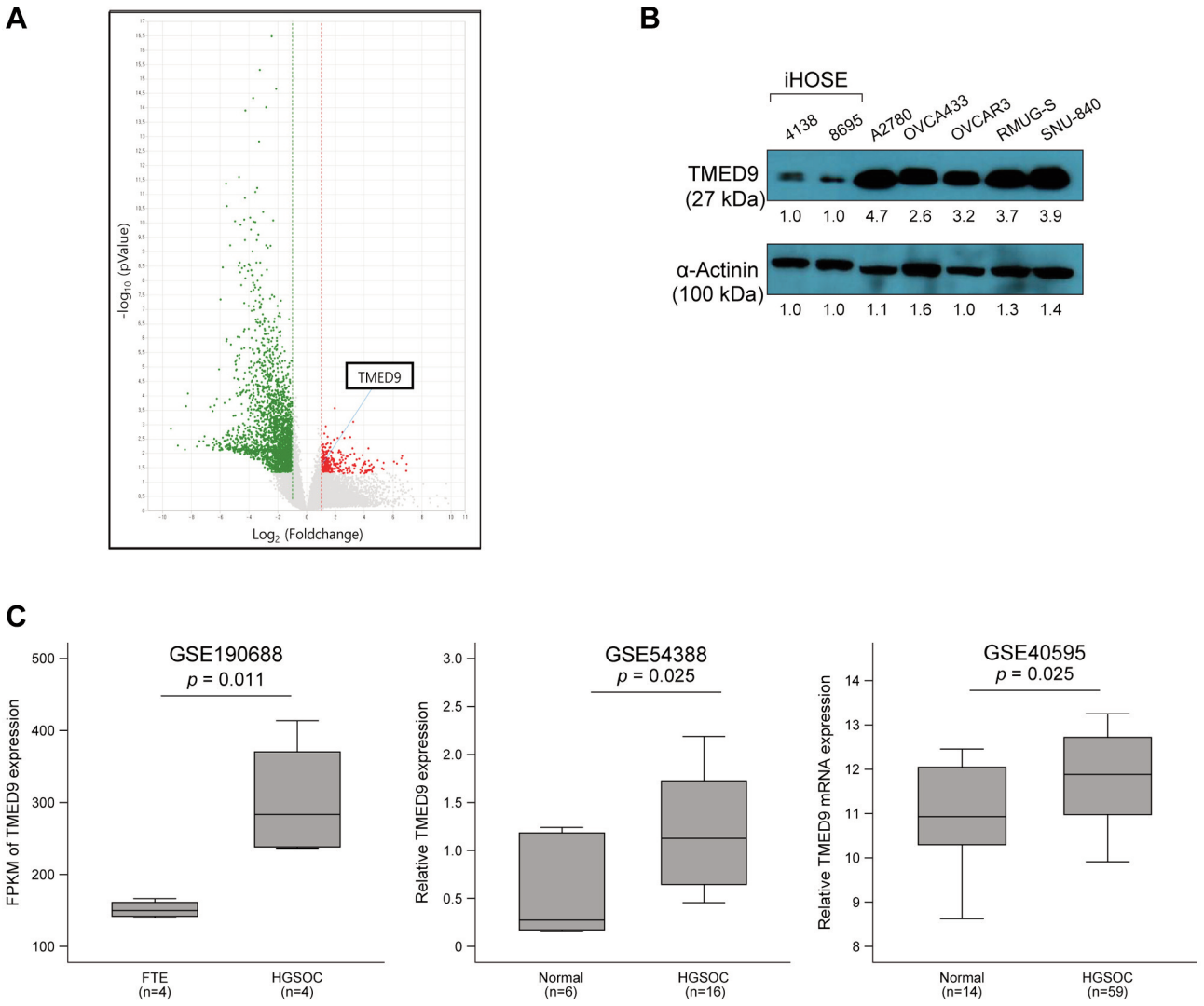


Figure 1. *Comparative analysis of Transmembrane Emp24 Domain-Containing protein 9 (TMED9) expression in epithelial ovarian cancer. A: Volcano plot of the distribution of differentially expressed genes between normal ovarian epithelial tissues and epithelial ovarian cancer (EOC) tissues in RNA sequencing analysis ($p<0.05$, and fold-change >2) showed the up-regulation of TMED9 in EOCs. The -log10 (p-value) for each gene is plotted against the log2 ratio of the intensity of its expression in cancer to that in normal tissue. Vertical dotted lines in red and green correspond to a 2.0-fold up-regulation and 2.0-fold down-regulation of expression, respectively. The green and red dots indicate genes differentially expressed at a significance level of $p=0.05$. Plots were generated using ExDEGA v.1.6.5 software (Ebiogen, Seoul, Republic of Korea). B: Expression of TMED9 protein in immortalized human ovarian epithelial cell lines (iHOSE 4138 and iHOSE 8695) and five ovarian cancer cell lines determined via western blotting. α-Actinin antibody was used as loading control. The numbers below each blot represent densitometric values. C: Box plots of the mRNA expression of TMED9 in normal and high-grade serous ovarian cancer (HGSOC) samples. Publicly available gene-expression data were obtained from the GEO database (GSE190688, GSE54388 and GSE40595). FPKM: Fragments per kilobase of transcript per million mapped reads; FTE: fallopian tube epithelium.*

Statistical analysis. TMED9 expression levels were evaluated using Mann–Whitney analysis or Kruskal–Wallis test, as necessary. OS and DFS were examined using the Kaplan–Meier technique. The hazard ratios (HR) and confidence intervals for the univariate and multivariate designs were also computed using the Cox proportional hazards approach. SPSS version 25.0 was used to conduct statistical analysis (IBM, Armonk, NY, USA). Statistical significance was defined as $p<0.05$ was considered statistically significant.

Results

Up-regulation of TMED9 in EOC. To evaluate *TMED9* mRNA expression in EOC, an RNA-seq was used to identify DEGs between normal ovarian epithelial tissues and HGSOC tissues. By using cDNA microarrays with 24,957 probe combinations, RNA extracted from tissues was directly

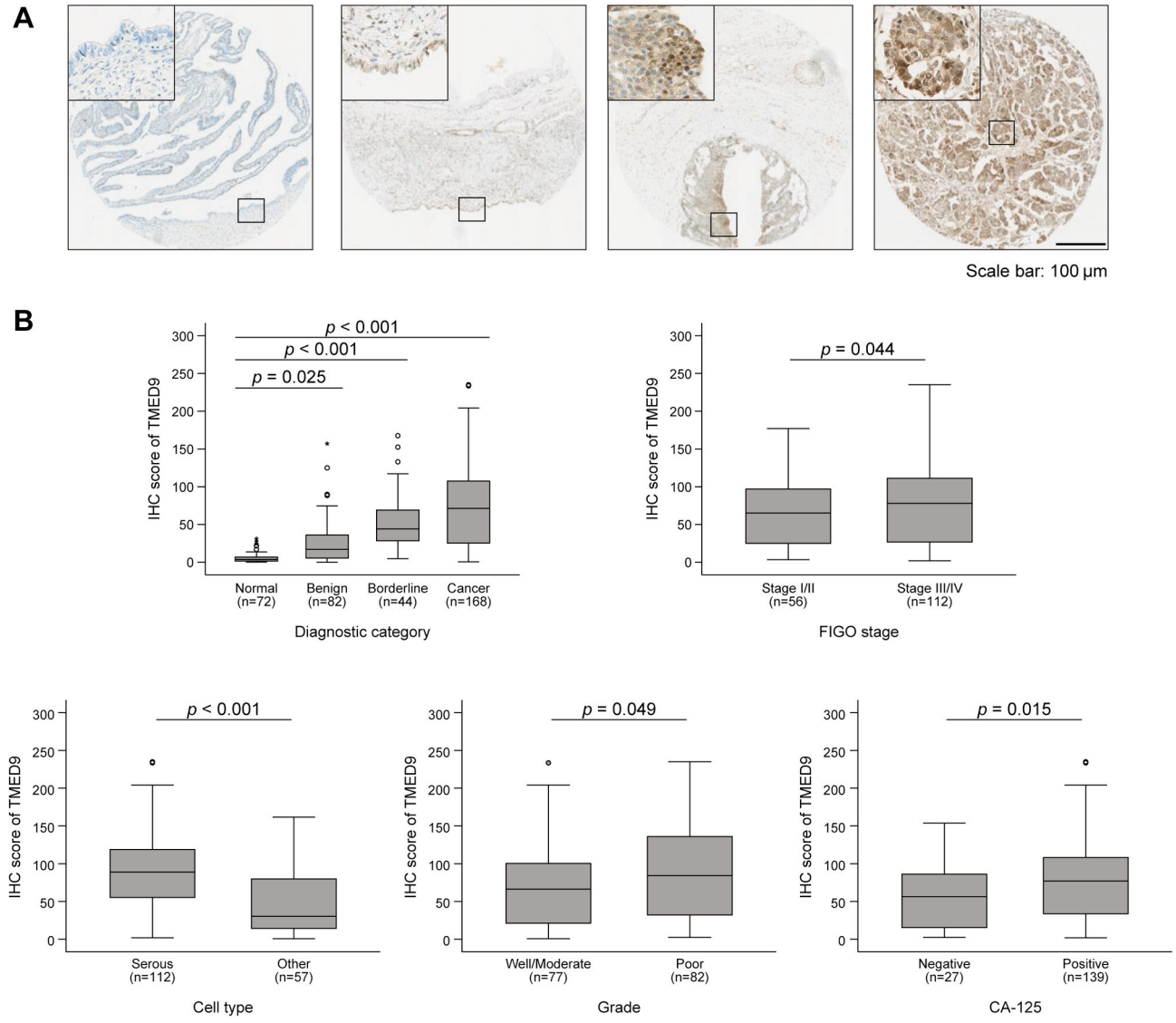


Figure 2. *Protein expression of transmembrane emp24 domain-containing protein 9 (TMED9) in epithelial ovarian cancer (EOC) and its association with clinicopathological characteristics. A: Representative immunohistochemical (IHC) staining images of TMED9 in non-adjacent ovarian epithelial tissues (normal), benign, borderline tumor, and EOCs. B: Box plots of TMED9 protein expression according to clinicopathological characteristics. FIGO: International Federation of Gynecology and Obstetrics; CA: cancer antigen. *Significantly different at p<0.05.*

compared. The volcano plot showed that 24,958 genes were DEGs ($p<0.05$, $\log_2$ fold-change>2) in cancer cells compared with normal epithelial tissues. We found that *TMED9* exhibited different expression patterns in HGSOCs compared to that of normal ovarian epithelial tissues (Figure 1A). The up-regulation of *TMED9* was further validated using publicly available datasets (*i.e.*, GSE190688, GSE54388, and GSE40595) and real-time polymerase chain reaction and immunoblotting in five ovarian cancer cell lines (namely A2780, OVCA433, OVCAR3, RMUG-S, and SNU840) relative to iHOSE control cells (Figure 1B and 1C). These findings collectively imply that TMED9 expression is increased in EOC.

Correlation between TMED9 protein expression and clinicopathological parameters of patients with EOC. Next, we compared the protein levels of TMED9 in non-adjacent normal epithelial tissues, benign, borderline, and EOC tissues through IHC. Compared to non-adjacent normal epithelial tissues, TMED9 protein levels gradually increased from normal tissues to EOCs. Representative IHC images are shown in Figure 2A. We found that TMED9 expression was

Table I. *Correlation between protein expression of TMED9 and clinicopathological characteristics of patients with epithelial ovarian cancer (n=366) determined by immunohistochemistry.*

Characteristic	Subgroup	Frequency (%)	Mean score (95% CI)	*p*-Value
Diagnostic category	Normal	72 (19.7)	5.59 (4.12-7.07)	<0.001
	Benign	82 (22.4)	24.75 (18.52-30.99)	
	Borderline	44 (12.0)	53.37 (42.07-64.66)	
	Cancer	168 (45.9)	77.09 (43.29-85.46)	
FIGO stage	I-II	56 (33.3)	66.49 (53.85-77.14)	0.044
	III-IV	112 (66.7)	83.58 (72.52-94.64)	
Cell type	Serous	112 (66.7)	91.49 (81.12-101.85)	<0.001
	Others	56 (33.3)	48.82 (37.56-60.07)	
Tumor grade	Well/Moderate	77 (48.4)	69.14 (52.22-81.07)	0.049
	Poor	82 (51.6)	86.48 (73.86-99.10)	
CA-125	Negative	27 (16.3)	53.67 (36.06-71.28)	0.015
	Positive	139 (83.7)	81.81 (72.44-91.17)	
Chemosensitivity	Sensitive	142 (92.8)	78.31 (68.78-87.84)	0.996
	Resistant	11 (7.2)	78.41 (48.93-107.88)	

CA: Cancer antigen; CI: confidence interval; FIGO: International Federation of Gynecology and Obstetrics.

strongly correlated with adverse clinicopathological features of EOC, including advanced FIGO stage (p=0.044), serous cell type (p<0.001), poor tumor grade (p=0.049), and elevated serum CA-125 level (p=0.015) (Table I and Figure 2B).

Relationship between TMED9 expression and prognosis in patients with EOC. The relevance of the predictive value of *TMED9* expression in patients with EOC was evaluated using Kaplan–Meier analysis after subdividing patients into high and low TEMD9 groups by the optimal cut-off point (determined by the maximum rank statistics as an immunohistochemistry score of >69.55). High *TMED9* expression was significantly associated with poor DFS and OS (both p<0.001, Figure 3A). Additionally, by analyzing Kaplan–Meier analysis by FIGO stage and utilizing information from http://kmplot.com, we validated the relevance and impact of impact of TMED9 on the prognosis of patients with EOC. Figure 3B shows that advanced FIGO stage (p<0.001) was associated with poor DFS and OS. As shown in Figure 3C, the DFS and OS of patients with high *TMED9* expression were significantly poorer than that of patients with low *TMED9* expression, which were in line with the results for our own cohort. Moreover, Cox multivariate analysis showed that high *TMED9* expression served as a standalone predictor of DFS (HR=1.93, 95% CI=1.22-3.05); p=0.005) and OS (HR=3.49, 95% C=1.69-7.21; p=0.001) (Table II). In summary, the data demonstrated that high *TMED9* expression might be a predictive biomarker for poor prognosis in patients with EOC.

Knockdown of TMED9 expression inhibits ovarian cancer cell proliferation, migration, and invasion. To assess the biological consequences of *TMED9* overexpression in ovarian cancer cells, *TMED9* was silenced using siRNA targeting *TMED9* (si*TMED9*) in OVCAR3 and OVCA433 cells. *TMED9* knockdown was verified by western blot (Figure 4A). Subsequently, we examined the effect of *TMED9* knockdown on the growth of EOC cells *in vitro*. Compared with siControl cells, knockdown of *TMED9* inhibited cell proliferation by 40% and 30% in OVCAR3 and OVCA433 cell lines, respectively (Figure 4B). Similarly, colony-formation assay showed that *TMED9* knockdown reduced the number of colonies formed (Figure 4C). Boyden chamber assays were performed to evaluate the role of *TMED9* in the migration and invasion of EOC cells. As shown in Figure 4D and E, silencing *TMED9* markedly reduced the migration and invasion of EOC cells. These data collectively demonstrate that the knockdown of *TMED9* prevents EOC cell migration, infiltration, and growth.

Discussion

Even though there has been significant advancement in EOC surgery and chemotherapy in past years, early detection of diseases is still difficult due to the absence of obvious symptoms and reliable screening procedures. Therefore, for the diagnosis and treatment of EOC, it is crucial to identify new and potent biomarkers linked to early diagnosis, and prognostic indicators.

The proteins in TMED/p24 family are responsible for innate immune signaling and the selection of cargo through the ER-Golgi network of proteins or secretory pathway (9, 26). Given this family's huge diversity of functions, abnormalities in the expression or instability of these proteins can contribute to disease development, such as cancer. For example, overexpression of *TMED3* was reported to act as an oncoprotein

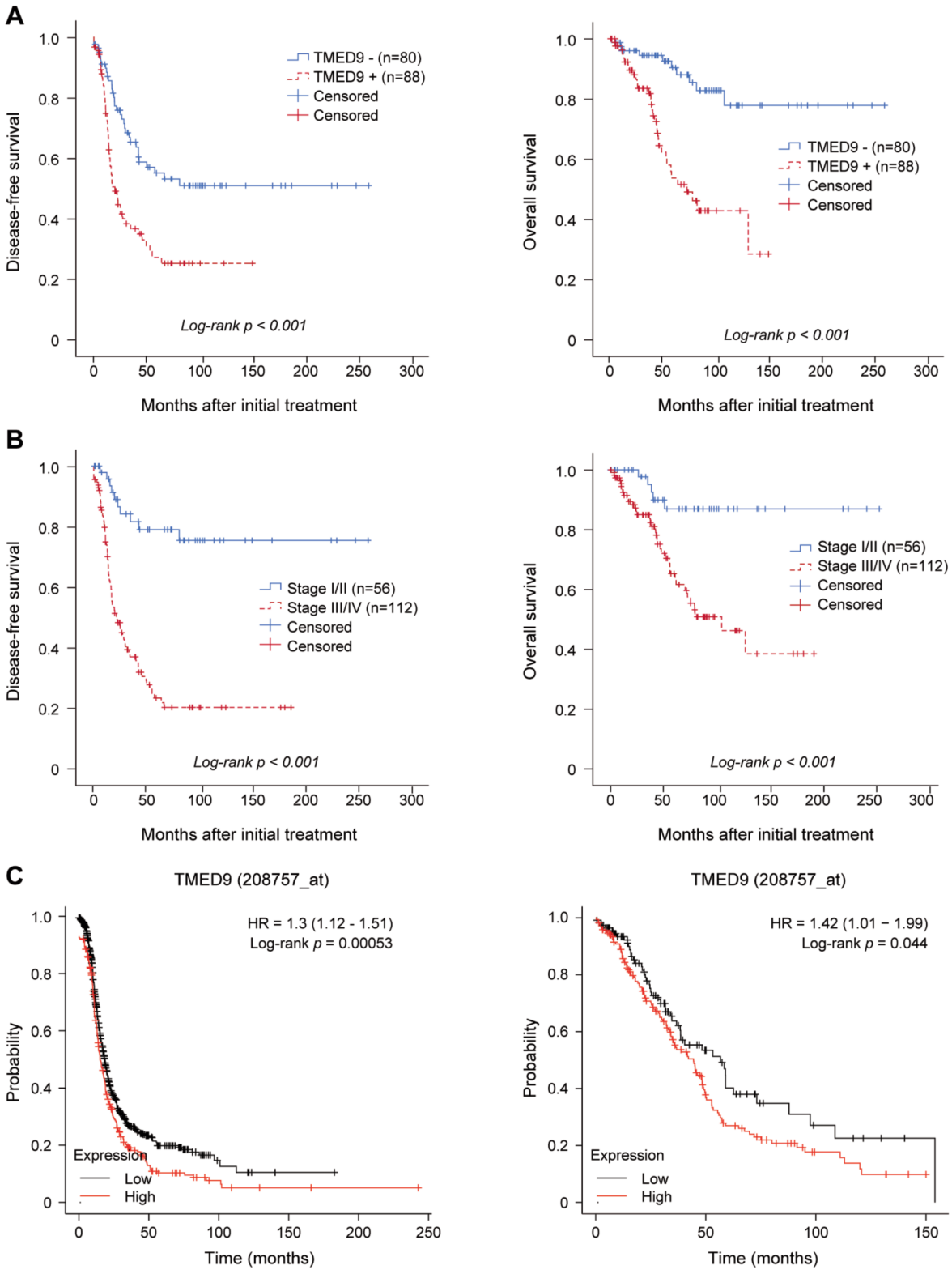


Figure 3. *Kaplan–Meier curve of survival of patients with epithelial ovarian cancer (EOC) according to transmembrane emp24 domain-containing protein 9 (TMED9) expression. A: Disease-free and overall survival of patients with epithelial ovarian cancer (EOC) analyzed according to TMED9 expression. B: Disease-free and overall survival of patients with EOC according to International Federation of Gynecology and Obstetrics stage. C: Analysis of prognosis according to the TMED9 expression in patients with EOC using data from http://kmplot.com. HR: Hazard ratio.*

Table II. *Univariate and multivariate analyses of the associations between prognostic factors and disease-free survival and overall survival in epithelial ovarian cancer.*

Prognostic factor		Disease-free survival				Overall survival			
		Univariate		Multivariate		Univariate		Multivariate	
		HR (CI)	*p*-Value	HR (CI)	*p*-Value	HR (CI)	*p*-Value	HR (CI)	*p*-Value
Age	>50 Years	1.58 (1.06-2.35)	**0.024**	0.92 (0.62-1.53)	0.915	2.12 (1.17-3.84)	**0.013**	1.33 (0.69-2.56)	0.385
FIGO stage	III-IV	6.42 (3.33-12.39)	**<0.001**	4.65 (2.28-9.48)	**<0.001**	5.10 (2.02-12.86)	**0.001**	3.29 (1.27-8.55)	**0.014**
Cell type	Serous	0.33 (0.2-0.55)	**<0.001**	0.51 (0.27-0.92)	**0.035**	0.22 (0.09-0.56)	**0.001**	0.40 (0.14-1.16)	0.091
Tumor grade	Poor	1.95 (1.28-2.97)	**0.002**	1.51 (0.96-2.36)	0.075	1.69 (0.95-3.00)	0.076	NA	
CA-125	>35 U/ml	2.39 (1.2-4.74)	**0.013**	0.90 (0.42-1.94)	0.790	2.22 (0.80-6.16)	0.127	NA	
TMED9	Positive[a]	2.28 (1.48-3.52)	**<0.001**	1.93 (1.22-3.05)	**0.005**	4.92(2.6-9.32)	**<0.001**	3.49 (1.69-7.21)	**0.001**

CA: Cancer antigen; CI: confidence interval; FIGO: International Federation of Gynecology and Obstetrics; NA: not applicable. [a]Cut-off value for TMED9 positivity was an immunohistochemistry score of >69.55. Statistically significant *p*-values are shown in bold.

in EOC, HCC, prostate cancer, breast cancer, and kidney malignancies, and was found to be a poor prognostic factor in individuals with EOC and breast cancer (26-31). However, the oncogenic roles of *TMED9* have only been demonstrated in colon cancer, HCC, breast cancer, and lower-grade glioma, not in EOC (11, 12, 32). Ju *et al*. reported the significant overexpression of *TMED9* in breast cancer tissues as a potential predictive biomarker for poor OS and DFS in HCC (12). Yang *et al*. observed that overexpression of *TMED9* at the mRNA and protein levels was significantly associated with advanced stage, vascular invasion, and poor prognosis (32). Consistent with these studies, our result also showed *TMED9* to be up-regulated in EOC compared to non-adjacent normal ovarian epithelial tissues, and this finding was further verified using The Cancer Genome Atlas and GEO datasets. TMED9 protein expression was markedly increased in EOCs compared to those in borderline, benign tumors, and non-adjacent normal epithelia. TMED9 expression was associated with advanced FIGO stage and elevated serum CA-125 level. Notably, high TMED9 expression was an independent prognostic factor for both OS and DFS in patients with EOC.

In addition, we further revealed the function of TMED9 in EOC cell lines. *TMED9* knockdown inhibited cell proliferation, colony formation, invasion, and migration of EOC cells. This result is consistent with previous findings. According to a study by Mishra *et al*. in colon cancer, TMED9 binds to the precursor of membranous forms of transforming growth factor α (TGFα) and regulates the expression of TGFα in membrane and coat protein complex II (COPII) secretory vesicles (11). Furthermore, it was reported that the expression of CNIH4, which regulates metastasis *via* the TGFα signaling pathway and is found in COPII secretory vesicles, is regulated by TMED9 activity in colon cancer (11). *TMED9* knockdown also reduced the secretion of TGFα in HCC cells as well as colon cancer cells. Additionally, Yang *et al*. confirmed that *TMED9* knockdown in HCC36 cells reduced expression of β-catenin, GLI1, and phosphorylation of extracellular-regulated kinase and signal transducer and activator of transcription 3, whilst its overexpression increased these (10), implying that CNIH4/TGFα/GLI1 and WNT-β-catenin mechanisms are involved in the advancement of HCC. The development of EOC is also influenced by the TGFα//GLI1 and WNT-β-catenin pathways (33), however, the relationship between CNIH4 and EOC has not yet been clarified. Therefore, additional research is required to clarify the mechanisms connecting TMED9 and CNIH4 and the associated signaling pathways.

In our study, we demonstrated that TMED9 protein expression was lowest in normal non-adjacent ovarian epithelial tissues, and its expression gradually increased from benign to borderline tumors and was expressed the highest in EOC. Overexpression of TMED9 positively correlated with adverse clinicopathological parameters and had an independent prognostic power for DFS and OS, further supporting its use as a valuable prognostic biomarker for EOC. While the signaling pathways associated with TMED9 need to be addressed in future studies, our *in vitro* studies in EOC cell lines showed a significant association of *TMED9* expression with proliferation, colony formation, migration, and invasion. Therefore, our findings strongly support the targeting of *TMED9* as a novel strategy for EOC treatment, and the overexpression of *TMED9* as a prognostic biomarker.

Conflicts of Interest

The Authors declare no conflicts of interest.

Authors' Contributions

Conceptualization, H.Y., G.H.H., J.-Y.C., and H.C.; methodology, G.H.H., J.-H.K., J.-Y.C., and H.C.; data curation, G.H.H., H.Y.; investigation, G.H.H., H.Y.; writing - original draft preparation, H.Y., G.H.H.; writing - review and editing, J.-Y.C., J.-H.K., and H.C. All Authors read and approved the final article.

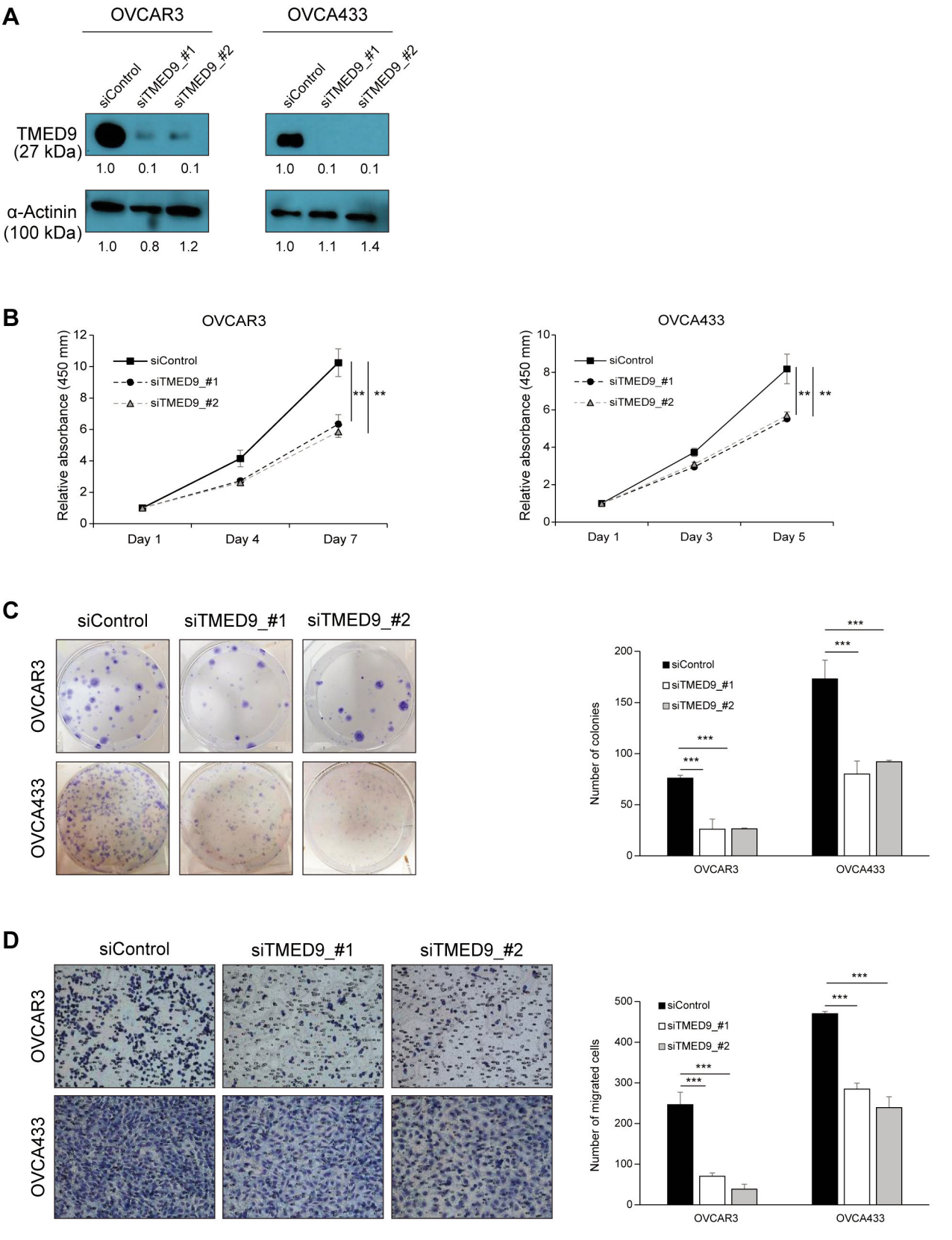


Figure 4. *Continued*

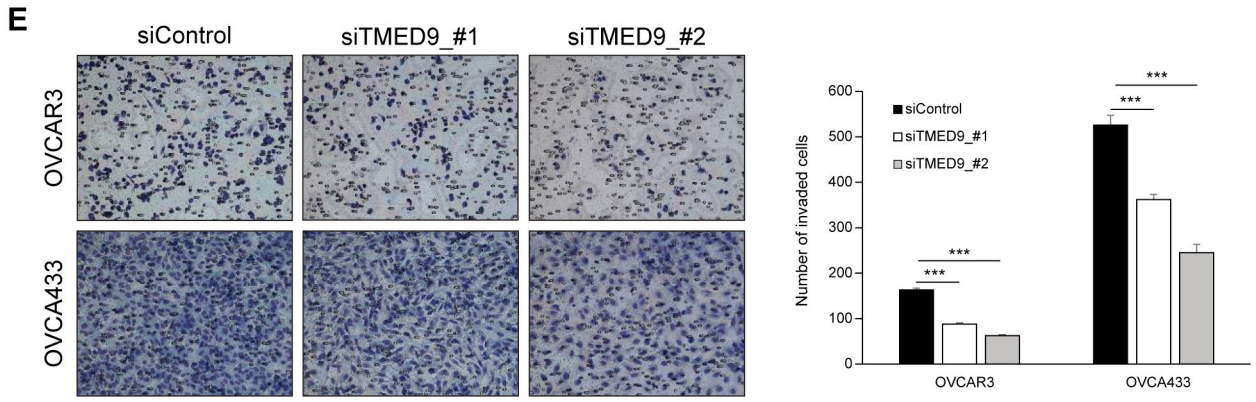


Figure 4. *The effects of transmembrane emp24 domain-containing protein 9 (TMED9) knockdown on cell proliferation, migration, and invasion in ovarian cancer cells. A: OVCAR3 and OVCA433 cells were transfected with siRNA against TMED9 for 48 h. Protein expressions of TMED9 and α-actinin were analyzed by western blot. The numbers below each blot represent densitometric values. B: Compared with cells transfected with siControl, siTMED9#1 and siTMED9#2 transfection significantly suppressed cell proliferation. C: Colony formation. D: Cell migration. E: Cell invasion. Significantly different at: **p<0.05 and ***p<0.005. Data are the mean±standard error of triplicate experiments.*

Acknowledgements

This study was supported by a National Research Foundation of Korea (NRF) grant funded by the Korean government (MIST) (NRF-2020R1A2C2004782). This research was supported by the Bio & Medical Technology Development Program of the National Research Foundation (NRF) funded by the Korean government (MSIT) (NRF-2017M3A9B8 069610). This study was also supported by a faculty research grant from the Yonsei University College of Medicine (No. 6-2020-0226).

References

1 Sung H, Ferlay J, Siegel RL, Laversanne M, Soerjomataram I, Jemal A and Bray F: Global Cancer Statistics 2020: GLOBOCAN estimates of incidence and mortality worldwide for 36 cancers in 185 countries. CA Cancer J Clin *71(3)*: 209-249, 2021. PMID: 33538338. DOI: 10.3322/caac.21660

2 Siegel RL, Miller KD, Fuchs HE and Jemal A: Cancer statistics, 2021. CA Cancer J Clin *71(1)*: 7-33, 2021. PMID: 33433946. DOI: 10.3322/caac.21654

3 Jung KW, Won YJ, Kang MJ, Kong HJ, Im JS and Seo HG: Prediction of cancer incidence and mortality in Korea, 2022. Cancer Res Treat *54(2)*: 345-351, 2022. PMID: 35313101. DOI: 10.4143/crt.2022.179

4 Lheureux S, Gourley C, Vergote I and Oza AM: Epithelial ovarian cancer. Lancet *393(10177)*: 1240-1253, 2019. PMID: 30910306. DOI: 10.1016/S0140-6736(18)32552-2

5 Perren TJ, Swart AM, Pfisterer J, Ledermann JA, Pujade-Lauraine E, Kristensen G, Carey MS, Beale P, Cervantes A, Kurzeder C, du Bois A, Sehouli J, Kimmig R, Stähle A, Collinson F, Essapen S, Gourley C, Lortholary A, Selle F, Mirza MR, Leminen A, Plante M, Stark D, Qian W, Parmar MK, Oza AM and ICON7 Investigators: A phase 3 trial of bevacizumab in ovarian cancer. N Engl J Med *365(26)*: 2484-2496, 2011. PMID: 22204725. DOI: 10.1056/NEJMoa1103799

6 Poveda A, Floquet A, Ledermann JA, Asher R, Penson RT, Oza AM, Korach J, Huzarski T, Pignata S, Friedlander M, Baldoni A, Park-Simon TW, Tamura K, Sonke GS, Lisyanskaya A, Kim JH, Filho EA, Milenkova T, Lowe ES, Rowe P, Vergote I, Pujade-Lauraine E and SOLO2/ENGOT-Ov21 investigators: Olaparib tablets as maintenance therapy in patients with platinum-sensitive relapsed ovarian cancer and a BRCA1/2 mutation (SOLO2/ENGOT-Ov21): a final analysis of a double-blind, randomised, placebo-controlled, phase 3 trial. Lancet Oncol *22(5)*: 620-631, 2021. PMID: 33743851. DOI: 10.1016/S1470-2045(21)00073-5

7 Strating JR and Martens GJ: The p24 family and selective transport processes at the ER-Golgi interface. Biol Cell *101(9)*: 495-509, 2009. PMID: 19566487. DOI: 10.1042/BC20080233

8 Aber R, Chan W, Mugisha S and Jerome-Majewska LA: Transmembrane emp24 domain proteins in development and disease. Genet Res (Camb) *101*: e14, 2019. PMID: 31878985. DOI: 10.1017/S0016672319000090

9 Anantharaman V and Aravind L: The GOLD domain, a novel protein module involved in Golgi function and secretion. Genome Biol *3(5)*: research0023, 2002. PMID: 12049664. DOI: 10.1186/gb-2002-3-5-research0023

10 Yang YC, Chien MH, Lai TC, Tung MC, Jan YH, Chang WM, Jung SM, Chen MH, Yeh CN and Hsiao M: Proteomics-based identification of TMED9 is linked to vascular invasion and poor prognoses in patients with hepatocellular carcinoma. J Biomed Sci *28(1)*: 29, 2021. PMID: 33888099. DOI: 10.1186/s12929-021-00727-5

11 Mishra S, Bernal C, Silvano M, Anand S and Ruiz I Altaba A: The protein secretion modulator TMED9 drives CNIH4/TGFα/GLI signaling opposing TMED3-WNT-TCF to promote colon cancer metastases. Oncogene *38(29)*: 5817-5837, 2019. PMID: 31253868. DOI: 10.1038/s41388-019-0845-z

12 Ju G, Xu C, Zeng K, Zhou T and Zang L: High expression of transmembrane P24 trafficking protein 9 predicts poor prognosis in breast carcinoma. Bioengineered *12(1)*: 8965-8979, 2021. PMID: 34635011. DOI: 10.1080/21655979.2021.1990673

13 Berek JS, Renz M, Kehoe S, Kumar L and Friedlander M: Cancer of the ovary, fallopian tube, and peritoneum: 2021 update. Int J Gynaecol Obstet *155(Suppl 1)*: 61-85, 2021. PMID: 34669199. DOI: 10.1002/ijgo.13878
14 Scully RE: World Health Organization classification and nomenclature of ovarian cancer. Natl Cancer Inst Monogr *42*: 5-7, 1975. PMID: 1234636.
15 Nishino M, Jagannathan JP, Ramaiya NH and Van den Abbeele AD: Revised RECIST guideline version 1.1: What oncologists want to know and what radiologists need to know. AJR Am J Roentgenol *195(2)*: 281-289, 2010. PMID: 20651182. DOI: 10.2214/AJR.09.4110
16 Bushnell B: BBMap. Available at: https://sourceforge.net/projects/bbmap [Last accessed on July 28, 2022]
17 Leggett RM, Ramirez-Gonzalez RH, Clavijo BJ, Waite D and Davey RP: Sequencing quality assessment tools to enable data-driven informatics for high throughput genomics. Front Genet *4*: 288, 2013. PMID: 24381581. DOI: 10.3389/fgene.2013.00288
18 Dobin A, Davis CA, Schlesinger F, Drenkow J, Zaleski C, Jha S, Batut P, Chaisson M and Gingeras TR: STAR: ultrafast universal RNA-seq aligner. Bioinformatics *29(1)*: 15-21, 2013. PMID: 23104886. DOI: 10.1093/bioinformatics/bts635
19 Anders S, Pyl PT and Huber W: HTSeq—a Python framework to work with high-throughput sequencing data. Bioinformatics *31(2)*: 166-169, 2015. PMID: 25260700. DOI: 10.1093/bioinformatics/btu638
20 Love MI, Huber W and Anders S: Moderated estimation of fold change and dispersion for RNA-seq data with DESeq2. Genome Biol *15(12)*: 550, 2014. PMID: 25516281. DOI: 10.1186/s13059-014-0550-8
21 Dou Z, Qiu C, Zhang X, Yao S, Zhao C, Wang Z, Chu R, Chen J, Chen Z, Li R, Wang K, Liu P, Liu C, Song K and Kong B: HJURP promotes malignant progression and mediates sensitivity to cisplatin and WEE1-inhibitor in serous ovarian cancer. Int J Biol Sci *18(3)*: 1188-1210, 2022. PMID: 35173547. DOI: 10.7150/ijbs.65589
22 Yeung TL, Leung CS, Wong KK, Gutierrez-Hartmann A, Kwong J, Gershenson DM and Mok SC: ELF3 is a negative regulator of epithelial-mesenchymal transition in ovarian cancer cells. Oncotarget *8(10)*: 16951-16963, 2017. PMID: 28199976. DOI: 10.18632/oncotarget.15208
23 Dasari S, Fang Y and Mitra AK: Cancer associated fibroblasts: Naughty neighbors that drive ovarian cancer progression. Cancers (Basel) *10(11)*: 406, 2018. PMID: 30380628. DOI: 10.3390/cancers10110406
24 Győrffy B, Lanczky A, Eklund AC, Denkert C, Budczies J, Li Q and Szallasi Z: An online survival analysis tool to rapidly assess the effect of 22,277 genes on breast cancer prognosis using microarray data of 1,809 patients. Breast Cancer Res Treat *123(3)*: 725-731, 2010. PMID: 20020197. DOI: 10.1007/s10549-009-0674-9
25 Shin HY, Yang W, Lee EJ, Han GH, Cho H, Chay DB and Kim JH: Establishment of five immortalized human ovarian surface epithelial cell lines via SV40 T antigen or HPV E6/E7 expression. PLoS One *13(10)*: e0205297, 2018. PMID: 30296284. DOI: 10.1371/journal.pone.0205297
26 Strating JR and Martens GJ: The p24 family and selective transport processes at the ER-Golgi interface. Biol Cell *101(9)*: 495-509, 2009. PMID: 19566487. DOI: 10.1042/BC20080233
27 Yang J, Huang H, Xiao D, Duan Y, Zheng Y and Chen Z: Knockdown of TMED3 inhibits cell viability and migration and increases apoptosis in human chordoma cells. Int J Oncol *58(5)*: 15, 2021. PMID: 33760171. DOI: 10.3892/ijo.2021.5195
28 Ha M, Moon H, Choi D, Kang W, Kim JH, Lee KJ, Park D, Kang CD, Oh SO, Han ME, Kim YH and Lee D: Prognostic role of *TMED3* in clear cell renal cell carcinoma: a retrospective multi-cohort analysis. Front Genet *10*: 355, 2019. PMID: 31057605. DOI: 10.3389/fgene.2019.00355
29 Vainio P, Mpindi JP, Kohonen P, Fey V, Mirtti T, Alanen KA, Perälä M, Kallioniemi O and Iljin K: High-throughput transcriptomic and RNAi analysis identifies AIM1, ERGIC1, TMED3 and TPX2 as potential drug targets in prostate cancer. PLoS One *7(6)*: e39801, 2012. PMID: 22761906. DOI: 10.1371/journal.pone.0039801
30 Pei J, Zhang J, Yang X, Wu Z, Sun C, Wang Z and Wang B: TMED3 promotes cell proliferation and motility in breast cancer and is negatively modulated by miR-188-3p. Cancer Cell Int *19*: 75, 2019. PMID: 30976199. DOI: 10.1186/s12935-019-0791-4
31 Zheng H, Yang Y, Han J, Jiang WH, Chen C, Wang MC, Gao R, Li S, Tian T, Wang J, Ma LJ, Ren H and Zhou WP: TMED3 promotes hepatocellular carcinoma progression via IL-11/STAT3 signaling. Sci Rep *6*: 37070, 2016. PMID: 27901021. DOI: 10.1038/srep37070
32 Yang YC, Chien MH, Lai TC, Tung MC, Jan YH, Chang WM, Jung SM, Chen MH, Yeh CN and Hsiao M: Proteomics-based identification of TMED9 is linked to vascular invasion and poor prognoses in patients with hepatocellular carcinoma. J Biomed Sci *28(1)*: 29, 2021. PMID: 33888099. DOI: 10.1186/s12929-021-00727-5
33 Smolle E, Taucher V, Pichler M, Petru E, Lax S and Haybaeck J: Targeting signaling pathways in epithelial ovarian cancer. Int J Mol Sci *14(5)*: 9536-9555, 2013. PMID: 23644885. DOI: 10.3390/ijms14059536

Received June 29, 2022
Revised July 23, 2022
Accepted July 28, 2022